Supplemental material to this article can be found at:
http://molpharm.aspetjournals.org/content/suppl/2023/01/20/molpharm.122.000638.DC1
1521-0111/103/4/241–254$35.00
MOLECULAR PHARMACOLOGY
dx.doi.org/10.1124/molpharm.122.000638
Mol Pharmacol 103:241–254, April 2023

A Novel Role of Uricosuric Agent Benzbromarone in BK Channel Activation and Reduction of Airway Smooth Muscle Contraction[S]

Jian Gao,[1] Hao Yin, Yanqun Dong, Xintong Wang, Yani Liu, and KeWei Wang

Department of Pharmacology, School of Pharmaceutical Sciences, Peking University, Beijing, China (J.G., X.W.); Department of Pharmacology, School of Pharmacy, Qingdao University Medical College, Qingdao, China (H.Y., Y.D., Y.L., K.W.); and Institute of Innovative Drugs, Qingdao University, Qingdao, China (Y.L., K.W.)

Received October 12, 2022; accepted December 19, 2022

ABSTRACT

The uricosuric drug benzbromarone, widely used for treatment of gout, hyperpolarizes the membrane potential of airway smooth muscle cells, but how it works remains unknown. Here we show a novel role of benzbromarone in activation of large conductance calcium-activated K^+ channels. Benzbromarone results in dose-dependent activation of macroscopic big potassium (BK) currents about 1.7- to 14.5-fold with an EC_{50} of 111 μM and shifts the voltage-dependent channel activation to a more hyperpolarizing direction about 10 to 54 mV in whole-cell patch clamp recordings. In single-channel recordings, benzbromarone decreases single BKα channel closed dwell time and increases the channel open probability. Coexpressing β1 subunit also enhances BK activation by benzbromarone with an EC_{50} of 67 μM and a leftward shift of conductance-voltage (G-V) curve about 44 to 138 mV. Site-directed mutagenesis reveals that a motif of three amino acids ^{329}RKK^{331} in the cytoplasmic linker between S6 and C-terminal regulator of potassium conductance (RCK) gating ring mediates the pharmacological activation of BK channels by benzbromarone. Further ex vivo assay shows that benzbromarone causes reduction of tracheal strip contraction. Taken together, our findings demonstrate that uricosuric benzbromarone activates BK channels through molecular mechanism of action involving the channel RKK motif of S6-RCK linker. Pharmacological activation of BK channel by benzbromarone causes reduction of tracheal strip contraction, holding a repurposing potential for asthma and pulmonary arterial hypertension or BK channelopathies.

SIGNIFICANCE STATEMENT

We describe a novel role of uricosuric agent benzbromarone in big potassium (BK) channel activation and relaxation of airway smooth muscle contraction. In this study, we find that benzbromarone is an activator of the large-conductance Ca^{2+}- and voltage-activated K^+ channel (BK channel), which serves numerous cellular functions, including control of smooth muscle contraction. Pharmacological activation of BK channel by the FDA-approved drug benzbromarone may hold repurposing potential for treatment of asthma and pulmonary arterial hypertension or BK channelopathies.

Introduction

The big potassium (BK) channel, also known as Maxi-K, is a voltage-gated and Ca^{2+}-activated potassium channel characterized by its large conductance of potassium ions across cell membrane, comprising four symmetric pore-forming α subunits (Yellen, 2002; Hite et al., 2017; Tao et al., 2017) with or without association of regulatory β (Garcia-Calvo et al., 1994; Brenner et al., 2000; Orio et al., 2002) or γ subunits (Yan and Aldrich, 2010; Zhang and Yan, 2014). The structure of each BKα subunit is featured with seven-transmembrane (TM) domains (S0–S6) and a large intracellular C terminus containing two regulators of conductance of K^+ (RCK) domains as Ca^{2+} sensor gating rings (Yellen, 2002; Yusifov et al., 2008; Zhang et al., 2010; Hite et al., 2017; Tao et al., 2017). The voltage sensing domains (VSDs) formed by S1 to S4 are activated by depolarization, and their subsequent movements result in the opening of pore domain formed by S5 and S6 (Ma et al., 2006). Two RCK domains bound by calcium are believed to open the channel by exerting pulling force on the passive spring S6-RCK1-linker (Niu et al., 2004). The VSD and the N-lobe of RCK1 are also found to contact each other by noncovalent interactions, allowing mutual modulation in addition to direct activation on the pore domain (Cox et al., 1997; Horrigan and Aldrich, 2002; Hite et al., 2017).

BK channels are abundantly expressed in smooth muscle cells and neurons, playing an important role in controlling

This work was supported by research grants awarded to K.W. from the National Natural Sciences Foundation of China [Grant 81573410], the Ministry of Science and Technology of China [Grant 2018ZX09711001-004-006], the Natural Sciences Foundation of Shandong Province [Grant ZR2015QL008], and the Science and Technology Program of Guangdong [Grant 2018B030334001].

No author has an actual or perceived conflict of interest with the contents of this article.

[1]Current affiliation: Washington University, St. Louis, Missouri.

dx.doi.org/10.1124/molpharm.122.000638.

[S] This article has supplemental material available at molpharm.aspetjournals.org.

ABBREVIATIONS: ACh, acetylcholine; benz, benzbromarone; BK, big potassium; CaCC, calcium-activated chloride channel; G-V, conductance-voltage; hBK, human BK; MCh, methacholine; PCR, polymerase chain reaction; PIP2, phosphatidylinositol 4, 5-bisphosphate; RCK, regulator of potassium conductance; RKK, for amino acids of Arginine 329, Lysine 330, and Lysine 331; TM, transmembrane; WT, wild-type.

cell membrane excitability (Latorre et al., 2017). BK channel activation modulates smooth muscle contractility by invoking the spontaneous transient outward potassium currents (STOCs) that hyperpolarize cell membrane potential (Bolton and Imaizumi, 1996; Hull et al., 2013). Activation of BK channels also contributes to repolarization of action potentials (Aps) and mediates the fast phase of fast afterhyperpolarization (fAHP) in neurons (Shao et al., 1999; Womack et al., 2009; Kimm et al., 2015). Functional deficit of BK channels is implicated in diseases such as epilepsy (Du et al., 2005; Lee and Cui, 2009), hypertension (Yang et al., 2013), urinary incontinence (Herrera et al., 2000; Hashitani and Brading, 2003; Meredith et al., 2004), and erectile dysfunction (González-Corrochano et al., 2013). Therefore, pharmacological activation of BK channels may hold promise for potential therapies, including asthma or pulmonary arterial hypertension (Vang et al., 2010), erectile disfunction (Boy et al., 2004), epilepsy (Boy et al., 2004; Lee and Cui, 2009; Vang et al., 2010), and brain ischemic stroke (Gribkoff et al., 2001).

Uricosuric agent benzbromarone is one of the most potent drugs for treatment of gout, a common type of arthritis that causes intensive pain and swelling in joints (Roddy and Doherty, 2010). Benzbromarone reduces serum urate level by inhibiting URAT-1 (Enomoto et al., 2002) and SLC2A9 (Caulfield et al., 2008) urate transporters located in the renal tubules, facilitating the dissolution of urate crystals. It is of interest that benzbromarone also inhibits the calcium-activated chloride channel (CaCC) ANO1/TMEM16A (Huang et al., 2012) and hyperpolarizes the membrane potential of airway smooth muscle cells (Danielsson et al., 2015). Some CaCC inhibitors such as tamoxifen (Duncan, 2005), niflumic acid, flufenamic acid, and NPPB (Gribkoff et al., 1996; Liu et al., 2015) can also activate BK channels. In addition, a structural analog of antiarrhythmic amiodarone (KB130015) also activates BK channels (Gessner et al., 2007). Based on the literature findings, we therefore hypothesized that uricosuric drug benzbromarone, a CaCC TMEM16A inhibitor, might also affect BK channels. To test this hypothesis, we investigated the effects of benzbromarone on BK channels with or without β subunits and contraction of constricted tracheal strips from mice. Our findings show that benzbromarone activates BK currents by interacting with the RKK motif of the channel S6-RCK1 linker. Benzbromarone also causes reduction of contracted tracheal strips, thus possessing therapeutic potential for asthma or diseases related to BK channel deficiency.

Materials and Methods

Chemicals and Solutions. Stock solutions of 100 mM benzbromarone from Aladdin (Shanghai, China), 100 mM Terbutaline from Aladdin, and 10 mM paxilline from Cayman (Ann Arbor, MI) in DMSO were stored at −20°C. Dilution to their final concentration in buffer was carried out immediately before use for electrophysiological recordings, with the highest concentration of compounds containing about DMSO about 0.3%. For ex vivo experiments, compounds were dissolved in the Krebs-Henseleit (K-H) buffer without DMSO. All other chemicals were of high grade (purity ≥98%) from Millipore-Sigma (St. Louis, MO).

Molecular Biology. Chinese hamster ovary (CHO) cells stably expressing human BK channel α subunits and β1 subunits (hBKα/β1) were used for subcloning. The cDNA of hBKα (gene accession number NM_001014797.2), expressed in smooth muscle tissue (McCobb et al., 1995), was subcloned into pcDNA3.1 (+) vector after reverse transcription. The translation of hBKα cDNA starts at the third ATG of hBKα cDNA that shares the same channel property as airway smooth muscle cells (Semenov et al., 2006; Lorca et al., 2014). Human BKβ1 (hBKβ1) was subcloned into vector pmCherry-N1, and the nucleotide sequence is identical to NM_004137.3.

The truncated BKα channel containing the N-terminal 342 residues without the gating ring of two tandem RCK1 and RCK2 (Budelli et al., 2013) was generated by polymerase chain reactions (PCRs) with forward primer (ACGCTAAGCTTATGGATGCGCTCATCATCC), reverse primer 1 (CACACAGAGATTC CTTAACTCCTCTTCCACTAACCGCACTATAGGA), and reverse primer 2 (CCGCTCGAGTCACACATCAGTTCCACACAGAGATTCCTTAACTCCT), using hBKα as the template with reverse primer 1 about 10% of reverse primer 2. A point mutation was introduced using Q5 polymerase for PCR, according to the manufacturer's instructions, and mutagenic oligonucleotides were purchased from Tsingke Biologic Technology (Beijing, China). Mutagenic primers consisted of reverse complimentary 15-mers before and after the codon representing the targeted amino acid, whereupon nonsynonymous mutations were introduced to the sequence by PCR as reported (Braman et al., 1996). Mutant clones were confirmed by sequencing at Tsingke Biologic Technology.

Sequence Alignment. The Sequence alignment was conducted by using NCBI cobalt (https://www.ncbi.nlm.nih.gov/tools/cobalt/re_cobalt.cgi) and NCBI blastp with BKα protein sequences NP_001014797.1 (human), NP_001380629.1 (rat), and Q08460.2 (mouse).

Cell Culture and Transfection. Chinese hamster ovary (CHO) cells or CHO cells stably expressing hBKα/β1 were cultured in F12 medium (F12; Invitrogen, Carlsbad, CA) supplemented with 10% fetal bovine serum (Gibco) and maintained at 37°C in a humidified atmosphere with 5% CO_2. CHO cells grown on 35-mm petri dishes were transfected with 1 μg construct cDNA of hBKα (or its mutants) alone or 0.25 μg hBKα (or its mutants) plus 0.75 μg auxiliary subunit using Lipofectamine 2000 (Invitrogen) 4 to 24 hours before patch-clamp experiments. Two hundred nanograms pEGFP-N1 was cotransfected for identification of transfected cells via fluorescence when needed.

Electrophysiology. Patch-clamp recordings were performed at room temperature of 20–24°C using an EPC-10 amplifier controlled via Patchmaster software (HEKA Elektronik). For whole-cell patch clamp recordings, the bath solution contained 140 mM KCl and 10 mM HEPES with pH adjusted to 7.4 using KOH. For the pipette solution, 10 mM EGTA was added for eliminating effect of intracellular calcium. For whole-cell recording condition at intracellular $[Ca^{2+}]_I$ = 300 nM, $CaCl_2$ was added into the pipette solution according to the WEBMAXC software (https://somapp.ucdmc.ucdavis.edu/pharmacology/bers/maxchelator/CaEGTA-TS.htm) before pH adjustment. For single-channel recordings in configuration of either on-cell patch or inside-out patch, the pipette solution was the same as the bath solution of whole-cell recordings. For whole-cell recordings, data were sampled at 50–100 kHz without low-pass filtering. Patch pipettes from borosilicate filaments had tip resistance of 3–5 MΩ. For on-cell single channel recordings, pipettes with tip resistance about 11 MΩ were used and data were sampled at 100 kHz and filtered at 1 kHz offline. Data for single-channel dwell time were collected and analyzed by pCLAMP 10.5 Software. Other data were collected and analyzed using Origin 8.0 Software. Drugs dissolved in the bath solution were perfused with an 8-Channel Valve Controlled Gravity Perfusion System (ALA Scientific Instruments).

Curve Fitting. The conductance (G) was derived from steady-state (peak) currents according to Ohm's law: $G = I/(V - E_K)$, where E_K = 0 mV in symmetrical $[K^+]$. Data were expressed as the means ± S.D. The conductance-voltage (G-V) curves from individual recordings were fitted with the Boltzmann equation: $G/G_{max} = 1/(1 + e^{(V_m - V_{0.5})/S})$, where $V_{0.5}$ is the voltage of half-maximum activation, S is the slope of the curve, V_m is the test potential, G is the conductance, and G_{max} is the maximal conductance. The mean values of current amplitude or mechanical force in response to benzbromarone

concentrations were fitted with the Hill equation: y = START + (END − START) * x^n/(k^n + x^n). For single-channel dwell time analysis, the average channel open or closed lifetimes (τ) were determined by fitting a single exponential distribution, $N(t)/N(0) = \exp(-t/\tau)$, where $N(t)$ denotes the number of channel opening or closing events with a lifetime longer than time t to each histogram.

Animals. All protocols describing animal care and experimental procedures are approved by the Animal Ethics Committee of Qingdao University (Qingdao, Shandong, China). Animal studies are reported in compliance with the ARRIVE guidelines (Kilkenny et al., 2010), and every effort aims to minimize animals' suffering. For our experiments, Sprague-Dawley rats (8 weeks old, male) were purchased from Beijing Vital River Laboratory Animal Technology Co., Ltd. (Beijing, China). They were housed in a pathogen-free environment at the Animals Housing Center of Qingdao University with proper ambient temperature (21°C) and a 12L:12D cycle and fed with a standard chow diet and water ad libitum.

Ex Vivo Measurements of Mouse Tracheal Strip Constriction. Isolated tracheal specimen assay was performed as previously described (Lai et al., 2013). Briefly, male Sprague-Dawley rats of 8 weeks old were asphyxiated with CO_2 for 3 to 4 minutes in a special chamber, and their tracheas were quickly removed below the pharynx and above the primary bronchus bifurcation. A tracheal tube was transferred into cold oxygenated Krebs-Henseleit (K-H) buffer and gently dissected clean of surrounding tissues. Held by a thin glass stick, the rat tracheal was cut into spiral strips with proper length before being attached to a force transducer by a metal hook being before placed in an oxygenated K-H buffer. Resting tension was readjusted to 1 g before being challenged with 10 μM methacholine (MCh) solution for 5 minutes. After the baseline was stable, tracheal strips were challenged with benzbromarone and 10 μM MCh. The tracheal strips were recorded for 5 minutes in response to each drug application.

To evaluate the degree of tracheal constriction, the contraction rate was calculated using the following equation: The relaxation rate (%) = [the force when acetylcholine (ACh) was used alone − the force when ACh and test drugs were combined]/the force when ACh was used alone * 100%.

Data Analysis and Statistics. All data were expressed as means ± S.D. and analyzed using GraphPad 5. Statistical difference was assessed using either paired t tests or one-way ANOVA. A value of $P < 0.05$ was considered to be statistically significant and denoted with an asterisk (*) or (#) in the text or figures. $P < 0.01$ was noted with (**) or (##), and $P < 0.001$ was marked with (***) or (###). A value of $P > 0.05$ was considered to be statistically insignificant and denoted with (ns) or (NS) in the figures.

Results

Activation of BKα Channels by Benzbromarone in Dose-Dependent Manner. We started examining the effect of benzbromarone on human BK pore-forming α subunits transiently expressed in CHO cells using whole-cell patch clamp assay. Perfusing different concentrations of benzbromarone (1–300 μM) resulted in a dose-dependent activation of BK currents about 1.7- to 14.5-fold in response to 100 mV membrane depolarization with an EC_{50} of 111 ± 15 μM and a Hill coefficient value of 1.1 ± 0.2 (Fig. 1A). The 300 μM benzbromarone-mediated current was inhibited by a specific BK channel inhibitor paxilline at 0.3 μM (Fig. 1B). As a blank control, benzbromarone had no effect on untransfected CHO cells (Supplemental Fig. 1).

To further examine the effect of benzbromarone on voltage-dependent activation of BKα channels, we recorded the current evoked by a range of potentials from −80 mV to 240 mV in 20-mV increments in the presence or absence of benzbromarone (Fig. 1C). Plotting the G-V curve revealed that benzbromarone at 10 μM and 100 μM led to the leftward shift of BKα channel activation about Δ10 mV and Δ54 mV, respectively, from the half-activation voltage ($V_{0.5}$) at 162 ± 18 mV (Fig. 1D; Table 1), and the benzbromarone-mediated effect on voltage-dependent activation of BKα was reversible upon washout (Fig. 1, C and D). These results indicate that benzbromarone acts as a BK channel activator.

Intracellular calcium concentration can vary from 100 nM to 1 μM under physiologic conditions. We tested the effect of benzbromarone on BKα activation under 300 nM $[Ca^{2+}]_i$. Benzbromarone (benz) caused the leftward shifts of BKα channel activation by about Δ9 mV(10 μM benz) and Δ53 mV(100 μM benz), respectively, from the half-activation voltage ($V_{0.5}$) at 124 ± 2 mV (Fig. 1E; Table 1) which suggests that physiologic intracellular calcium does not influence the effect of benzbromarone on BKα.

Leftward Shift for Voltage-Dependent Activation of BKα Channels Coexpressed with β1 by Benzbromarone. Because auxiliary subunits can alter BK channel gating and pharmacology, we further tested the effect of benzbromarone on BKα/β1 channel complexes. Similarly, benzbromarone dose dependently activated BKα/β1 currents at 100 mV with an EC_{50} of 67 ± 7 μM and a Hill coefficient value of 1.6 ± 0.2, and the activated current was completely inhibited by paxilline at 0.3 μM (Fig. 2, A and B). Application of benzbromarone at 10 and 100 μM caused the voltage-dependent activation of BKα/β1 currents with larger leftward shifts about Δ44 mV and Δ138 mV, respectively (Fig. 2, C and D). Comparing the $V_{0.5}$ of BK channel with or without β1 subunit, benzbromarone resulted in a larger left shift of voltage dependence of BKα/β1 complex activation (Fig. 2E), further demonstrating the effect of uricosuric agent benzbromarone on activating BK currents in the presence of auxiliary β1 subunits.

Increase of BKα or BKα/β1 Complex Single-Channel Open Probability by Benzbromarone. To further confirm and characterize the on-target effect of benzbromarone on BK channel, we recorded BKα single-channel currents in on-cell patch configuration, ensuring that the cell membrane and intracellular environment were intact. At holding potential of +100 mV on the intracellular side, benzbromarone at 10 μM and 100 μM increased BKα single-channel open probability (Po) of 2.4- and 27.0-fold, respectively, compared with the control group (Fig. 3, A–E). Benzbromarone had no effect on the unitary single channel conductance (Fig. 3F). Analysis of distribution of open interval duration revealed that benzbromarone at 100 μM increased the channel open time by increasing τ_{open} about 2.3 times (Fig. 3G). Benzbromarone at 10 and 100 μM also decreased the channel closed interval duration by decreasing the τ_{closed} about 2.8 and 14.0 times, respectively (Fig. 3H). These results indicate that benzbromarone activates BK channel mainly through destabilizing the channel closed state and stabilizing the channel open state.

We also examined the effect of benzbromarone on single-channel currents of BKα/β1 channel complexes. As shown in Fig. 4, A–F, the single-channel currents were recorded before and after 10 or 100 μM benzbromarone treatment, exhibiting an increased open probability without noticeable change of unitary single channel conductance. The mean open interval duration (τ_{open}) showed an increase about 1.6-fold in response to 100 μM benzbromarone (Fig. 4G). The closed interval

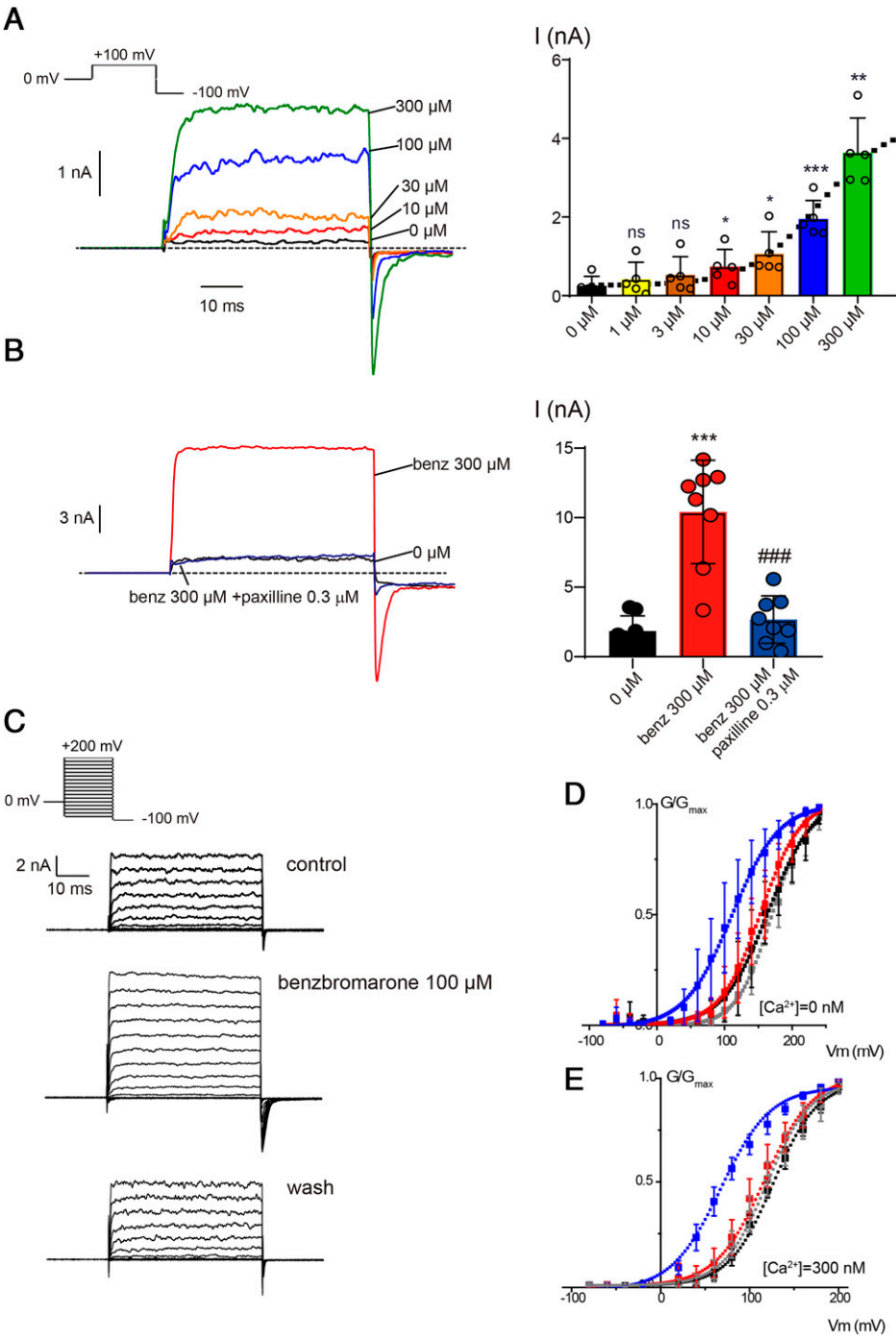

Fig. 1. Dose-dependent activation of macroscopic BK_{Ca} currents in CHO cells transiently transfected with *hslo1* by benzbromarone in whole-cell patch clamp assay. (A) Left panel: representative traces of BKα currents evoked from a holding potential at 0 mV to 100 mV, followed by a repolarizing voltage at −100 mV to elicit tail currents in the presence of different concentrations (1–300 μM) of benzbromarone; the dashed line indicates 0 current. Right panel: concentration-dependent fold increase of BK_{Ca} currents recorded at +100 mV in response to benzbromarone. $^{*}P < 0.05$, $^{**}P < 0.01$, $^{*}P < 0.001$ vs. basal currents in the absence of benzbromarone. One-way ANOVA with Tukey's multiple comparisons test. Data are expressed as the means ± S.D. ($n = 5$). The dashed line is fitted to Hill equation. (B) Left: representative current traces recorded in CHO cells expressing BKα channels before and after paxilline at 0.3 μM using the single depolarization pulse as indicated in panel A; the dashed line indicates 0 current. Right: summary data for left panel ($n = 8$). $^{***}P < 0.001$ vs. the control (0 μM) group. $^{\#\#\#}P < 0.001$ vs. the 300 μM benzbromarone group. Paired t test. (C) Currents evoked from −80 to +200 mV in 20 mV steps from a holding potential at 0 mV without intracellular calcium. Top and middle panels: whole-cell currents recorded before and after 100 μM benzbromarone. Bottom panel: current recorded after washout of benzbromarone. (D and E) Summary for G-V curves before (black), during benzbromarone of 10 μM (red) and 100 μM (blue), and after washing out of the compound (gray) with indicated intracellular Ca^{2+} concentrations. Dashed lines are fitted to Boltzmann. Data are expressed as the means ± S.D. ($n = 6$ for both conditions).

duration (τ_{closed}) was decreased about 2.0-fold and 23.3-fold by 10 and 100 μM benzbromarone, respectively (Fig. 4H), which was further confirmed by inside-out patch recordings (Supplemental Fig. 2). These results are also consistent with the observation on aforementioned BKα alone.

TABLE 1
Parameters for Boltzmann fitting of G-V curves

Construct	V0.5 (mV)			Slope Factor (mV)		
	Control	Benz 10	Benz 100	Control	Benz 10	Benz 100
BKα	161.5 ± 18.3	152.0 ± 17.4	107.6 ± 25.2	31.4 ± 6.0	28.9 ± 1.8	30.9 ± 3.6
BKα/β1	173.9 ± 8.6	129.9 ± 11.8	36.3 ± 28.1	31.2 ± 7.4	30.4 ± 4.2	31.2 ± 8.9
Truncated BKα	218.3 ± 16.4	200.0 ± 11.3	139.5 ± 27.0	37.2 ± 7.5	36.7 ± 7.0	40.5 ± 4.7
Truncated BKα + β1	239.2 ± 35.1	166.0 ± 18.4	72.7 ± 24.4	39.4 ± 7.1	40.6 ± 1.9	43.2 ± 5.5
BKα (9A9)	114.1 ± 13.2	97.0 ± 22.2	37.5 ± 25.5	34.3 ± 3.9	33.6 ± 1.5	32.0 ± 3.0
R11D	209.8 ± 10.3	160.9 ± 8.9	47.2 ± 32.5	37.8 ± 1.9	36.5 ± 0.7	42.3 ± 9.2
Truncated BKα RKK/AAA	84.4 ± 18.5	83.6 ± 13.3	81.9 ± 16.1	47.9 ± 6.0	37.3 ± 4.8	37.1 ± 4.1
BKα (300 nM Ca_i^{2+})	124.3 ± 2.4	115.1 ± 4.2	71.1 ± 7.9	27.5 ± 2.3	28.4 ± 3.4	29.9 ± 1.2
Truncated BKα (R329A)	218.3 ± 17.2	196.2 ± 16.8	156.3 ± 16.1	39.1 ± 11.4	34.5 ± 9.3	37.8 ± 4.1
Truncated BKα (K330A)	169.1 ± 6.3	141.0 ± 16.2	94.5 ± 7.8	36.3 ± 6.0	31.0 ± 3.3	23.3 ± 6.2
Truncated BKα (K331A)	227.3 ± 14.4	201.6 ± 16.2	159.8 ± 27.9	33.1 ± 6.9	30.8 ± 3.4	37.0 ± 1.7
Truncated BKα RKK/AAA + β1	92.0 ± 8.2	74.6 ± 5.4	−32.0 ± 23.6	25.6 ± 5.3	29.7 ± 5.3	27.5 ± 13.0
Truncated BKα E321A/E324A	147.5 ± 25.6	127.8 ± 7.3	76.3 ± 18.4	40.5 ± 3.9	39.8 ± 2.7	40.9 ± 9.2

Benz, benzbromarone in 10 or 100 μM.

Identification of the RKK Motif in the S6-RCK1 Linker Critical for BK Channel Activation by Benzbromarone. To identify the molecular determinant critical for benzbromarone-mediated BK activation, we generated a C-terminal truncated BKα channel lacking the two tandem RCK1 and RCK2 domains of the gating ring (Budelli et al., 2013) (Fig. 5A), and the truncated BKα exhibits a larger slope factor than wild-type (WT) BKα channels (Zhang et al., 2017). As shown in Fig. 5, B and C, benzbromarone at 10 and 100 μM increased the truncated BKα channel current and left shifted the G-V curve about 18 mV and 79 mV, respectively, compared with the control of $V_{0.5}$ (218 ± 16 mV), which is similar to the leftward shift of full-length BKα channel activation by benzbromarone (Fig. 5F). Similarly, benzbromarone at 10 and 100 μM also caused a left shift of the G-V curve of the truncated BKα coexpressed with β1 (Fig. 5, D and E) in a similar extent as WT BKα/β1 (Fig. 5G). These results suggest that benzbromarone activates BK channel by interacting with the amino acids from the N terminus to S6-RCK1 linker.

To further identify molecular determinants critical for benzbromarone-mediated channel activation, we generated several BK channel mutants and tested their effects in response to benzbromarone. As shown in Figs. 6A and 7E, the channel mutant 9A9 (G327L, N328S, K330N, Y332F), known to reduce the channel sensitivity to BK activator NS1619 or Cym04 (Gessner et al., 2012), retained the sensitivity to voltage-dependent activation in response to benzbromarone at 10 μM and 100 μM. Similarly, mutating β1 (R11D), which reduces the channel sensitivity to activation of phosphatidylinositol 4,5-bisphosphate (PIP2) (Tian et al., 2015) and DHA (Hoshi et al., 2013a), also retained the channel activation by benzbromarone (Figs. 6B and 7G). In contrast, a triple mutation in the RKK motif (^{329}RKK^{331} to AAA) of truncated BKα abolished the left shift of voltage-dependent channel activation by benzbromarone (Fig. 6, C and D). At the single-channel level, the triple mutant (^{329}RKK^{331} to AAA) had no significant change of single-channel open probability (Fig. 6E) and the open or closed dwell time (Fig. 6, F and G) in response to benzbromarone at 10 and 100 μM. These results demonstrate that benzbromarone activates BK channel currents through interacting with the RKK motif in the S6-RCK linker of BK channels.

To further explore any residue within the RKK motif important for benzbromarone-mediated effect, we generated three individual mutations of R329A, K330A, and K331A. As shown in Fig. 7, A–C and E, none of the mutants significantly reduced the leftward shift of voltage-dependent activation of BK currents by benzbromarone. Similarly, we also examined a double mutant of E321A/E324A that still remained in the leftward shift of BK currents by benzbromarone (Fig. 7, D and E). In contrast, coexpressing β1 subunit with truncated BKα triple mutant (RKK to AAA) rescued the leftward shift of BK activation by benzbromarone, which is similar to that of wild-type (WT) BKα/β1 (Fig. 7, F and G; Table 1).

Benzbromarone Reduces Tracheal Contraction via BK Channel Activation. To evaluate whether BK channel activator benzbromarone had any effect on airway smooth muscle contraction, we used a rat ex vivo model of tracheal spiral strip constriction induced by methacholine (MCh) and tested the effect of benzbromarone on branchial relaxation. As shown in Fig. 8a, benzbromarone at 100 μM resulted in the complete remission of 10 μM MCh-induced constriction, which was rapidly reversed by coapplication of BK channel inhibitor paxilline (10 μM). However, this reverse was difficult to sustain, possibly because paxilline caused a reversible inhibition of channel currents (Sanchez and McManus, 1996). The dose-response relationship demonstrated that bath application of different concentrations of benzbromarone ranging from 1 μM to 300 μM resulted in concentration-dependent relaxation of MCh-induced constriction of tracheal strips with an IC_{50} of 3.0 ± 0.9 μM and a Hill coefficient of 0.7 ± 0.2 (Fig. 8B). These results showed that pharmacological activation of BK channels by benzbromarone can dilate the constricted tracheal strips.

Discussion

Benzbromarone Activates BK Channel. Pharmacological activation of BK channels reduces cellular excitability, which is considered to be a promising strategy for treatment of diseases such as asthma, arterial hypertension, and stroke (Latorre et al., 2017). Based on literature findings that BK channels are abundantly expressed in smooth muscle cells and a US Food and Drug Administration (FDA)-approved uricosuric agent benzbromarone hyperpolarizes airway

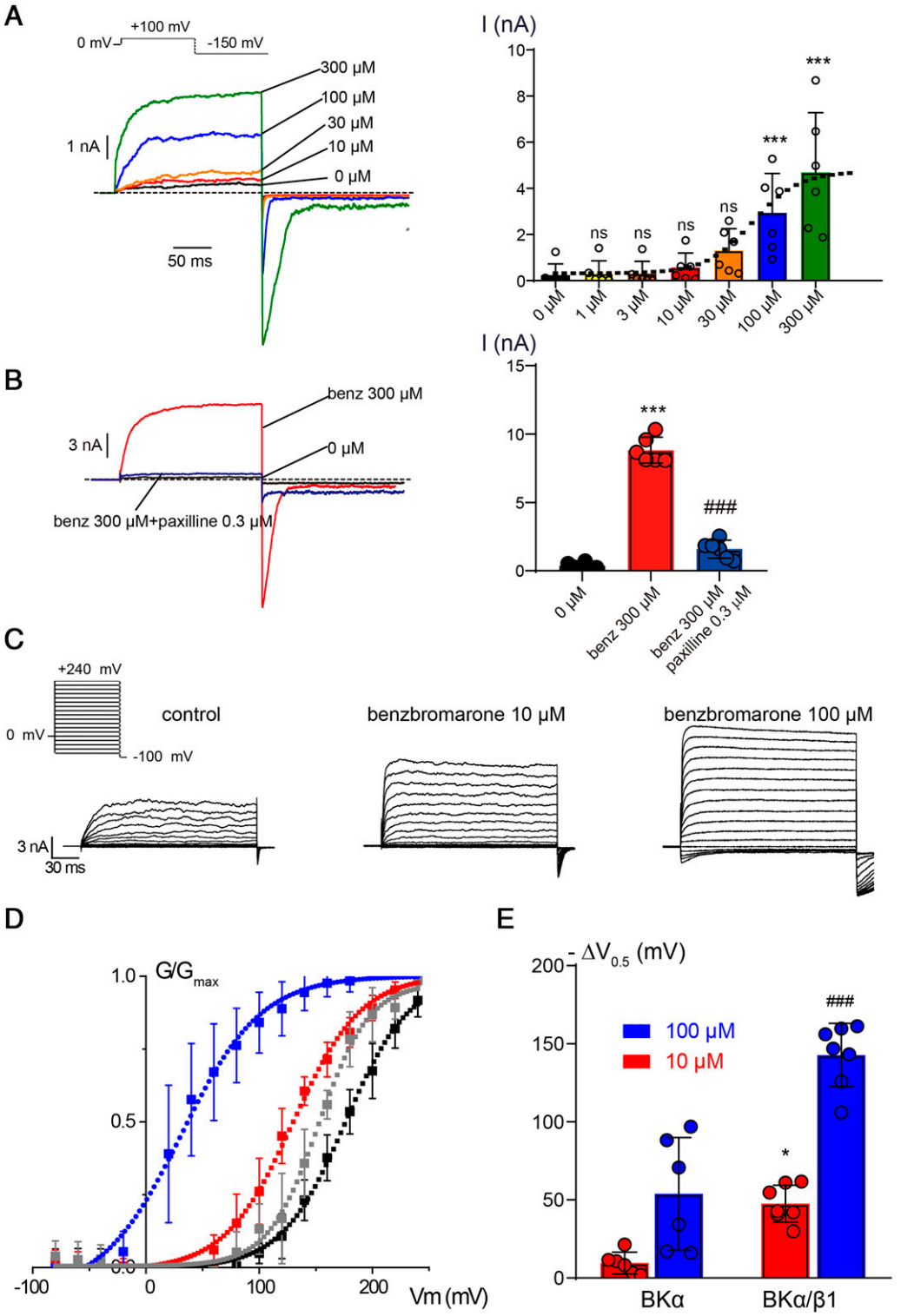

Fig. 2. Dose-dependent activation of macroscopic BK_{Ca} currents in CHO cells cotransfected with BKα/β1 by benzbromarone. (A) Left: representative traces of BKα + β1 currents evoked from a holding potential at 0 mV to 100 mV before change of voltage to −150 mV for eliciting tail currents in the presence of different concentrations of benzbromarone; the dashed line indicates 0 current. Right: concentration-response relationship for benzbromarone on BK_{Ca} currents recorded at +100 mV. *$P < 0.05$ vs. basal currents in the absence of benzbromarone. #$P < 0.05$ vs. currents evoked by 300 μM benzbromarone. One-way ANOVA. Data are presented as the means ± S.D. (n = 5 to 6). The dashed line is fitted for dose-response with Hill equation. (B) Left: representative BKα/β1 channel current traces recorded in CHO cells expressing BKα/β1 channels before and after application of paxilline at 0.3 μM using the single depolarization pulse as indicated in panel A; the dashed line indicates 0 current. Right: summary data for left panel (n = 6). Summary data are expressed as the means ± S.D. ***$P < 0.001$ vs. the control group. ###$P < 0.001$ vs. the 300 μM benzbromarone group. Paired t test. (C) Representative traces of BKα + β1 currents evoked from −80 to +240 mV in 20-mV incremental steps from a holding potential at 0 mV in the absence (left) or presence of benzbromarone: 10 μM (middle) and 100 μM (right) without intracellular calcium. (D) Summary for G-V curves from panel (C) before (black), during applications of benzbromarone at 10 μM (red) and 100 μM (blue), and after washout (gray). Dashed lines indicate Boltzmann fitting. Data are expressed as the means ± S.D. (n = 5). (E) Summary for the effect of benzbromarone on voltage-dependent activation of BK_{Ca} channels. *$P < 0.05$ vs. with $\Delta V_{0.5}$ value of BKα caused by 10 μM benzbromarone. ###$P <$ 0.001 vs. with $-\Delta V_{0.5}$ value of BKα caused by 100 μM benzbromarone. One-way ANOVA with Tukey's multiple comparisons test.

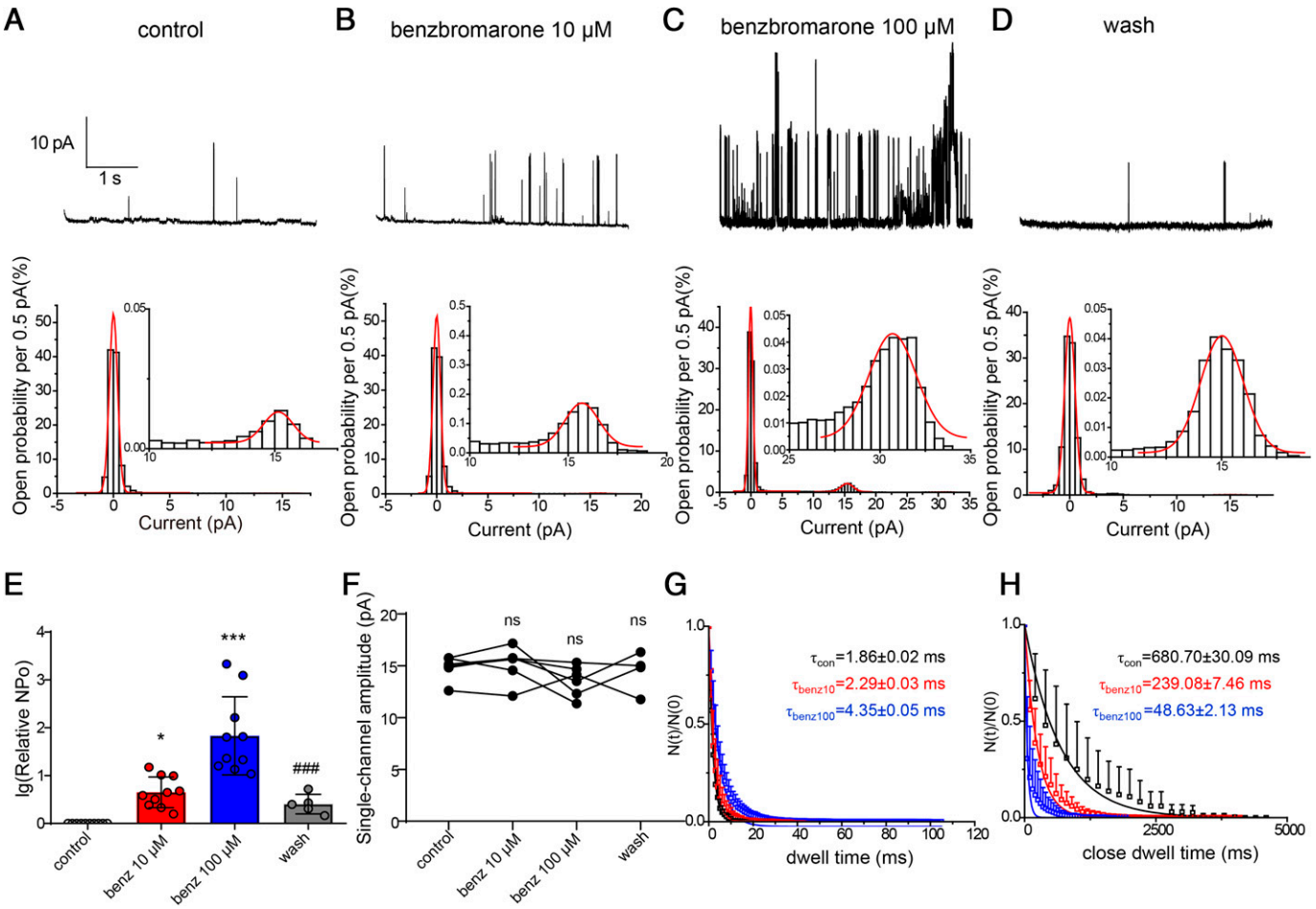

Fig. 3. Increase of BKα single-channel open probability by benzbromarone. (A–D) Representative single-channel currents recorded at +100 mV with indicated concentrations (10 and 100 μM) of benzbromarone before and after washout (upper panels). All-point histograms of single-channel events at the indicated concentrations of benzbromarone are shown in their bottom panels. The superimposed curves represent the fitting with Gaussian function. (E) Summary for open channel probability before and after applications of 10 and 100 μM benzbromarone (benz) and the washout of the compound (n = 5–10). *P < 0.05, ***P < 0.001 vs. the control group. #P < 0.05 vs. benz 100 μM group. One-way ANOVA with Tukey's multiple comparisons test. (F) Summary of single-channel current vs. their corresponding benzbromarone concentration (n = 4–6). ns (not significant), compared with the control group. One-way ANOVA with Tukey's multiple comparisons test. (G and H) Lifetime distributions of open and closed dwell times, plotted as survivor plots, are fitted by a single exponential distribution at each concentration of benzbromarone. Lines denote fitting of a single exponential distribution to the data (n = 4). Data are expressed as the means ± S.D.

smooth muscle cells (Danielsson et al., 2015; Miner et al., 2019), together with antiarrhythmic amiodarone derivative KB130015 that activates BK channels (Gessner et al., 2007), we in this study postulated that benzbromarone might also activate BK potassium channels. Here we show a previously unknown role of benzbromarone in pharmacological activation of BK channels, involving functional interaction in the RKK motif of the channel S6-RCK linker and also reducing the airway smooth muscle contraction. These key findings suggest that benzbromarone as a BK channel activator may hold repurposing potential for treatment of asthma, pulmonary arterial hypertension, or BK channel deficiency–related disease (Latorre et al., 2017).

The mechanism of action for benzbromarone is featured by the following: First, benzbromarone causes a significant left shift of voltage-dependent activation of both BKα and BKα/β1 complexes to hyperpolarizing direction, mainly by reducing the channel closed time. Second, auxiliary β1 subunit is specifically expressed in smooth muscle cells (Bhattarai et al., 2014), and coexpressing β1 subunit can further enhance the benzbromarone-mediated channel activation, suggesting more specific and better efficacy of benzbromarone likely for conditions related to smooth muscle cell dysfunction. Third, the ^{329}RKK^{331} motif within the S6-RCK linker mediates the pharmacological activation of BK channels by benzbromarone, suggesting that targeting the segment of S6-RCK linker may lead to identification of more diversified and specific small molecules for modulation of the channel pharmacology (Gessner et al., 2012). Finally, benzbromarone is mechanistically distinct from other BK channel activators such as lithocholic acid (Bukiya et al., 2011), arachidonic acid (Martín et al., 2014) and 17β-estradiol (Valverde et al., 1999), which are unable to activate BKα channel without β1 subunits. Benzbromarone is also different in comparison with the agonist GoSlo-SR-5-6, which is independent on regulation of β1 subunit (Kshatri et al., 2017). In contrast, benzbromarone behaves similarly to activators such as KB130015 (Gessner et al., 2007), DHA, and

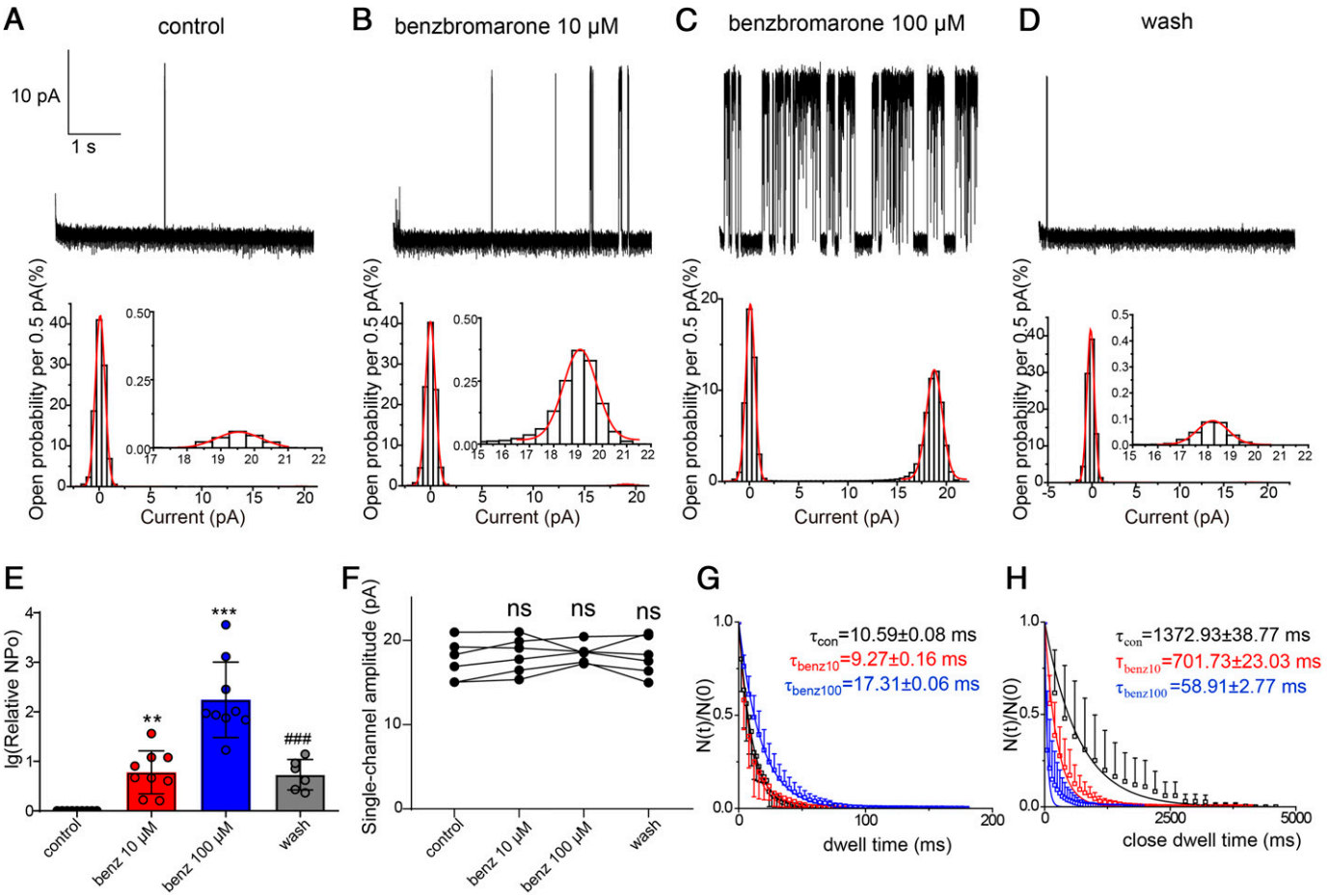

Fig. 4. Increase of single-channel open probability of BKα/β1 channel complexes by benzbromarone. (A–D) Representative traces of single-channel currents recorded at +100 mV with indicated concentrations of benzbromarone (upper panels). All-point histograms of single-channel events at the indicated concentrations of benzbromarone are shown in their bottom panels. The insets are superimposed curves from fittings of Gaussian function. (E) Summary for single-channel open probability before and after application of 10 or 100 μM benzbromarone and washout (n = 6–9). *P < 0.05 vs. the control group. #P < 0.05 vs. benzbromarone 100 μM group. One-way ANOVA with Tukey's multiple comparisons test. (F) Summary for single-channel current amplitude at their corresponding benzbromarone concentrations (n = 5). ns (not significant), P > 0.05 vs. the control group. One-way ANOVA with Tukey's multiple comparisons test. (G and H) Lifetime distributions for open (G) and closed (H) dwell times at 10 μM (red lines) and 100 μM (blue lines) of benzbromarone are fitted by a single exponential function (n = 3). Data are expressed as the means ± S.D.

PIP2 (Tian et al., 2015), with their activation effects dependent on β1 subunits.

The RKK Motif of the S6-RCK Linker Is Critical for Pharmacological Activation of BK Channels. The RKK motif of S6-RCK linker in BK channel has previously been shown to be a binding site of essential membrane lipid phosphatidylinositol 4,5-bisphosphate (PIP2) (Vaithianathan et al., 2008) as well as a binding site for two residues E321 and E324 from neighboring subunit (Tian et al., 2019). Both benzbromarone and PIP2 can destabilize the close state of channel, whereas β1 subunit potentiates their activation (Tian et al., 2015). Interestingly, benzbromarone works differently, as auxiliary β1 can only rescue benzbromarone-mediated effect on the ^{329}RKK^{331}/AAA mutant (Fig. 7, F and G) but not PIP2 (Vaithianathan et al., 2008; Tian et al., 2015).

Regulation of BK channels by auxiliary β subunits gives rise to functional diversity and tissue specificity. The recent cryogenic electronic microscopy (cryo-EM) structures of BK in complex with β4 reveals that four two-TM β4 subunits encircle BKα through multiple and simultaneous contacts between one α subunit and adjacent another α subunit (Tao and MacKinnon, 2019), thus forming a peripheral "tetrameric clamp" that enhances trafficking and surface expression. Interestingly, the bottom of TM1 of β4 near the intracellular membrane interface makes contacts between the S6-RCK linker of one α subunit and multiple S2-S3 linker and S0 regions from adjacent α subunit, thus indicating a critical role of S6-RCK linker segment in channel gating (Tao and MacKinnon, 2019) and regulating channel sensitivity to structurally diversified modulators such as DHA (Hoshi et al., 2013b), GoSlo-SR-5-6 (Webb et al., 2015), and cym04 (Gessner et al., 2012).

Comparing the Structural Diversity of Available Compounds May Lead to Identification of More Potent and Selective BK Activators. There are no BK activators that have been approved for clinical use. Up to date, several compounds in clinical trials, including BMS-204352, have been discontinued (Latorre et al., 2017) due to lack of clinical benefits over placebos (Kaczorowski and Garcia, 2016). BK activator andolast entered phase III clinical trial in 2015 for

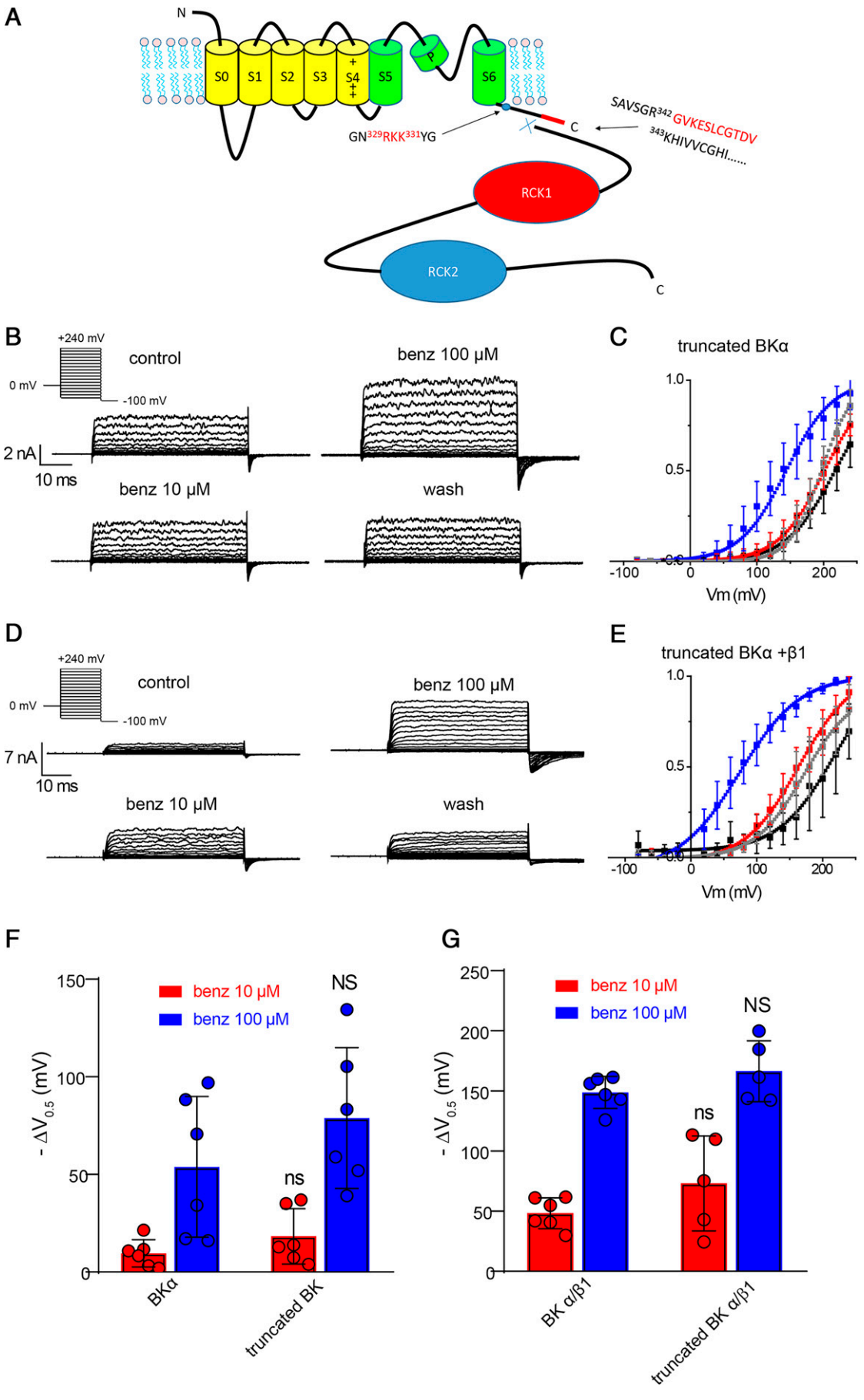
A
N
S0
S1
S2
S3
S4
S5
P
S6
C
GN329RKK331YG
SAVSGR342 GVKESLCGTDV
343KHIVVCGHI.....
RCK1
RCK2
C
B
+240 mV
0 mV
-100 mV
control
benz 100 µM
2 nA
10 ms
benz 10 µM
wash
C
truncated BKα
1.0
0.5
0.0
-100
0
100
200
Vm (mV)
D
+240 mV
0 mV
-100 mV
control
benz 100 µM
7 nA
10 ms
benz 10 µM
wash
E
truncated BKα +β1
1.0
0.5
0.0
-100
0
100
200
Vm (mV)
F
150
100
50
0
- ΔV0.5 (mV)
benz 10 µM
benz 100 µM
NS
ns
BKα
truncated BK
G
250
200
150
100
50
0
- ΔV0.5 (mV)
benz 10 µM
benz 100 µM
NS
ns
BK α/β1
truncated BK α/β1

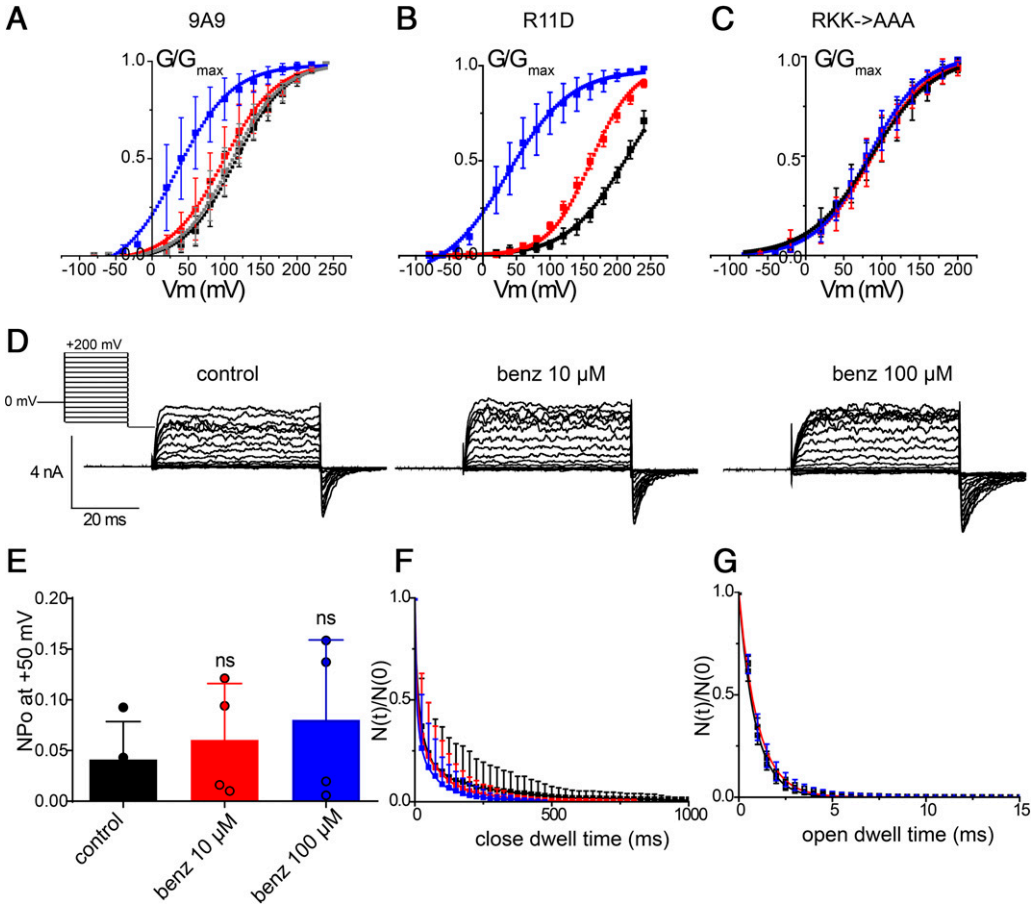

Fig. 6. Mutating the RKK motif in S6-C-linker abolishes benzbromarone-mediated activation of BK channels. (A) G-V curves of 9A9 channel mutant before (black) and after 10 μM (red) and 100 μM (blue) benzbromarone. (B) G-V curves of truncated BKα and R11D in β1 before (black) and after administrating 10 (red) and 100 μM (blue) benzbromarone. (C) G-V curve of the triple R329A/K330A/K331A mutation of truncated BKα before (black) and after application of 10 (red) and 100 μM (blue) benzbromarone. (D) Representative traces of whole-cell patch recordings of the triple R329A/K330A/K331A mutation truncated BKα channels before and after benzbromarone (benz) from panel (C). (E) Channel open probability (NPo) values before (black) and after application of 10 (red) and 100 μM (blue) benzbromarone at the voltage of +50 mV in on-cell patch recordings (n = 4). ns (not significant), $P > 0.05$ vs. the control group. (F and G) Lifetime distributions of closed dwell time and open dwell time before (black) and after administrating 10 (red) and 100 μM (blue) benzbromarone (n = 4).

treatment of asthma and chronic obstructive pulmonary disease (Mushtaq, 2014), but there is no further information or report yet since then. Antiarrhythmic amiodarone inhibits cardiac type 1 human ether-a-go-go-related gene (hERG1) potassium channels without significant effect on BK channels, and its derivative KB130015, like its parent compound, blocks hERG but activates BK channels (Gessner et al., 2007). Comparing the chemical structures of amiodarone, KB130015, and benzbromarone reveals that amiodarone contains an n-butyl group and a triethylamine group that are structurally different from the corresponding groups in benzbromarone or KB130015 (Fig. 9), suggesting that retaining the common groups in the structures of benzbromarone or KB130015 may be important for BK activation. Thus, further structural modifications of benzbromarone may lead to identification of more potent and selective BK channel activators.

Repurposing Multitargeting Benzbromarone Can Be More Beneficial for Asthma with Fewer Side Effects. Previous in vitro and ex vivo studies show that uricosuric agent benzbromarone acts on multiple molecular targets, including inhibition of Ca^{2+}-activated Cl^- channel ANO1/TMEM16A (Huang et al., 2012; Zhang et al., 2013; Danielsson et al., 2015; Miner et al., 2019) and activation of Kv7/KCNQ channels (Zheng et al., 2015). In the airway smooth muscles where BK, ANO1, and Kv7 channels are expressed, we speculate that benzbromarone, with multimechanism of action involving activation of BK and Kv7 channels and inhibition of TMEM16A channels for synergistic hyperpolarization of smooth muscle cells, may be more beneficial for treatment of

Fig. 5. Activation of C terminus–truncated BKα channel without RCK domains by benzbromarone. (A) Topological illustration of a BKα subunit with identical amino acid sequence as Slo1C-Kv-minT without the intracellular C terminus. (B–E) Truncated BKα without β1 (B) or with β1 (D) currents elicited by different concentrations (10 and 100 μM) of benzbromarone before and after washout. Summary for G-V curves of truncated BKα without β1 (C) or with β1 (E) before (black), during benzbromarone of 10 μM (red) or 100 μM (blue), and after washout (gray). Dashed lines indicate Boltzmann fitting to the data. Data are expressed as the means ± S.D. (n = 6). (F) Summary for $-\Delta V_{0.5}$ of truncated BKα channel or full-length BKα channel induced by 10 μM (red) or 100 μM (blue) benzbromarone. (G) Summary for leftward shift of $V_{0.5}$ for truncated BKα/β1 channel complexes or full-length BKα/β1 channel complexes elicited by 10 μM (red) or 100 μM (blue) benzbromarone. $P > 0.05$ vs. the left column (red). NS (not significant), $P > 0.05$ vs. the left column (blue). One-way ANOVA with Tukey's multiple comparisons test.

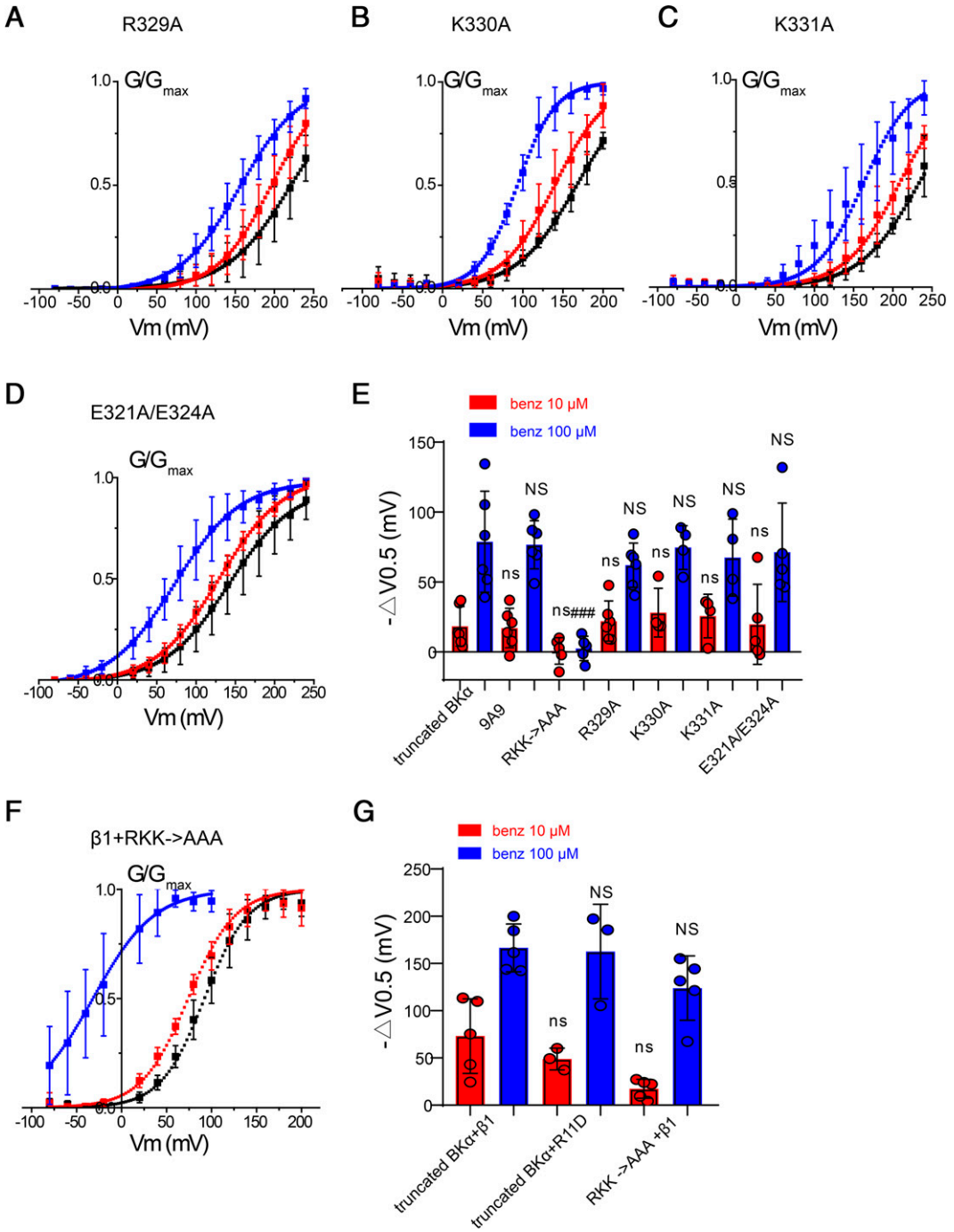

Fig. 7. Mutating individual residue of the RKK motif retains the activation of BK channel by benzbromarone. (A–C) G-V curves of R329A, K330A, and K331A in truncated BKα before (black) and after administration of 10 μM (red) and 100 μM (blue) benzbromarone. (D) G-V curves of mutant E321A/E324A in truncated BKα before (black) and after 10 μM (red) and 100 μM (blue) benzbromarone. (E) Summary for $-\Delta V_{0.5}$ of BKα and truncated BKα mutants caused by 10 μM and 100 μM benzbromarone. (F) G-V curves of R329A/K330A/K331A in truncated BKα coexpressed with β1 subunit before (black) and after administration of 10 μM (red) and 100 μM (blue) benzbromarone. (G) Summary for $-\Delta V_{0.5}$ of truncated BKα mutants and β1 caused by 10 μM and 100 μM benzbromarone. In (E) and (G) ns (not significant), $P > 0.05$, compared with the first red column on the left. ###$P < 0.001$ and NS (not significant), $P > 0.05$, vs. the first blue column on the left. One-way ANOVA with Tukey's multiple comparisons test.

asthma with fewer side effects. Similarly, because these targets are also expressional in tissues such as bladder, vascular smooth muscle, and dorsal root ganglion (DRG) neurons (Passmore et al., 2003; Greenwood and Ohya, 2009; Cho et al., 2012; Anderson et al., 2013; Zhang et al., 2013; Bijos et al., 2014; Heinze et al., 2014; Haick and Byron, 2016; Latorre et al., 2017; Du et al., 2018), benzbromarone may also possess repurposing potential for treatment of bladder overreactivity, periphery nociception, and vascular hypertension.

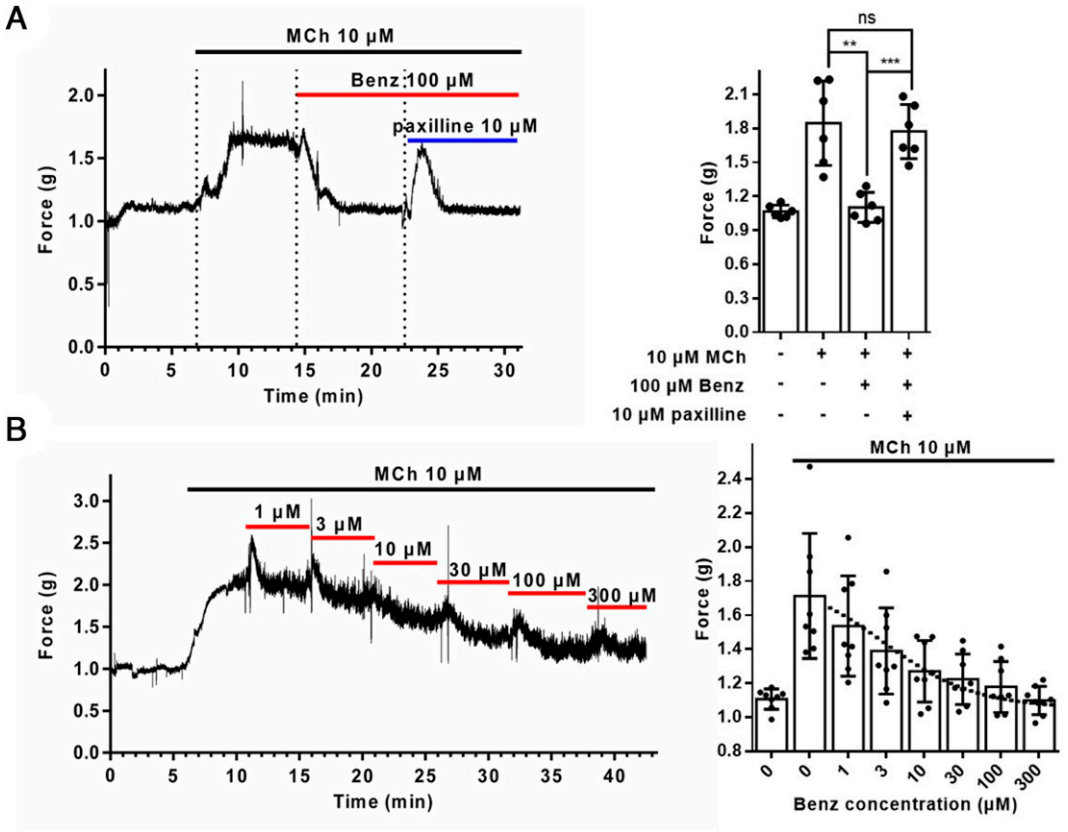

Fig. 8. Reduction of rat tracheal strip contraction by benzbromarone. (A) Left panel: time course for tracheal spiral strip contraction induced by 10 μM methacholine (MCh) in the presence and absence of 100 μM benzbromarone (Benz) or 100 μM benzbromarone with 10 μM paxilline. Right panel: summary for benzbromarone-induced reduction on contracted tracheal smooth muscles and the reversal by BK channel inhibitor paxilline. Data are expressed as the means ± S.D. ($n = 6$). *$P < 0.05$, **$P < 0.01$, ***$P < 0.001$. One-way ANOVA with Tukey's multiple comparisons test. (B) Left panel: time course for MCh-induced contraction of tracheal spiral strips in the presence of different concentrations of benzbromarone (1–300 μM). Right panel: summary for dose-dependent relaxation of MCh-induced contraction of tracheal spiral strips. Data are expressed as the means ± S.D. ($n = 8$). The dashed line is fitted with Hill equation.

We notice an existence of pharmacological overlap between BK channel activators and TMEM16A inhibitors. Also, a cluster of drugs such as rottlerin (mallotoxin), BMS-204352, and GoSlo function as activators for both BK and KCNQ channels (Schrøder et al., 2003; Manville and Abbott, 2018; Zavaritskaya et al., 2020). Although the underlying mechanism for this overlap is still unknown, our discovery of benzbromarone as a BK activator suggests a common activation mechanism shared by several channels such as BK, TMEM16A, and KCNQ channels (Danahay et al., 2020).

Benzbromarone is tolerable with poor penetration of the blood-brain barrier (Reinders et al., 2009; Zheng et al., 2015), rendering fewer concerns for adverse drug reactions such as depression and learning/memory impairment, likely involved in potent activation of neuronal BK channels. Clinical PK studies demonstrate that oral benzbromarone also exhibits high bioavailability in patients (Walter-Sack et al., 1988). Therefore, repurposing benzbromarone may represent an effective and safe strategy for therapy of asthma and pulmonary arterial hypertension.

Authorship Contributions

Participated in research design: X. Wang, K. Wang.

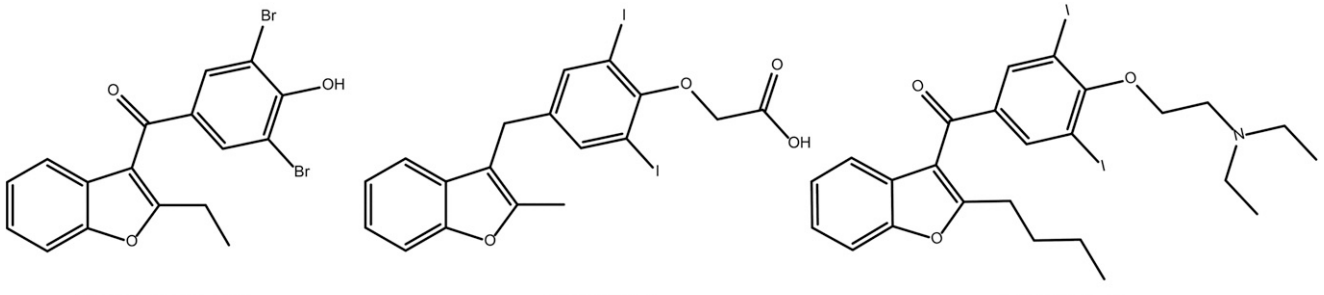

Fig. 9. Structural comparisons among benzbromarone analogs. Two-dimensional chemical structures of benzbromarone, KB130015, and amiodarone.

Conducted experiments: Gao, Yin, Dong, X. Wang.
Performed data analysis: Gao, Yin, Dong, X. Wang.
Wrote or contributed to the writing of the manuscript: Gao, Liu, K. Wang.

References

Anderson UA, Carson C, Johnston L, Joshi S, Gurney AM, and McCloskey KD (2013) Functional expression of KCNQ (Kv7) channels in guinea pig bladder smooth muscle and their contribution to spontaneous activity. *Br J Pharmacol* **169**:1290–1304.

Bhattarai Y, Fernandes R, Kadrofske MM, Lockwood LR, Galligan JJ, and Xu H (2014) Western blot analysis of BK channel β1-subunit expression should be interpreted cautiously when using commercially available antibodies. *Physiol Rep* **2**:e12189.

Bijos DA, Drake MJ, and Vahabi B (2014) Anoctamin-1 in the juvenile rat urinary bladder. *PLoS One* **9**:e106190.

Bolton TB and Imaizumi Y (1996) Spontaneous transient outward currents in smooth muscle cells. *Cell Calcium* **20**:141–152.

Boy KM, Guernon JM, Sit SY, Xie K, Hewawasam P, Boissard CG, Dworetzky SI, Natale J, Gribkoff VK, Lodge N, et al. (2004) 3-Thio-quinolinone maxi-K openers for the treatment of erectile dysfunction. *Bioorg Med Chem Lett* **14**:5089–5093.

Braman J, Papworth C, and Greener A (1996) Site-directed mutagenesis using double-stranded plasmid DNA templates. *Methods Mol Biol* **57**:31–44.

Brenner R, Jegla TJ, Wickenden A, Liu Y, and Aldrich RW (2000) Cloning and functional characterization of novel large conductance calcium-activated potassium channel beta subunits, hKCNMB3 and hKCNMB4. *J Biol Chem* **275**:6453–6461.

Budelli G, Geng Y, Butler A, Magleby KL, and Salkoff L (2013) Properties of Slo1 K+ channels with and without the gating ring. *Proc Natl Acad Sci USA* **110**:16657–16662.

Bukiya AN, Singh AK, Parrill AL, and Dopico AM (2011) The steroid interaction site in transmembrane domain 2 of the large conductance, voltage- and calcium-gated potassium (BK) channel accessory β1 subunit. *Proc Natl Acad Sci USA* **108**: 20207–20212.

Caulfield MJ, Munroe PB, O'Neill D, Witkowska K, Charchar FJ, Doblado M, Evans S, Eyheramendy S, Onipinla A, Howard P, et al. (2008) SLC2A9 is a high-capacity urate transporter in humans. *PLoS Med* **5**:e197.

Cho H, Yang YD, Lee J, Lee B, Kim T, Jang Y, Back SK, Na HS, Harfe BD, Wang F, et al. (2012) The calcium-activated chloride channel anoctamin 1 acts as a heat sensor in nociceptive neurons. *Nat Neurosci* **15**:1015–1021.

Cox DH, Cui J, and Aldrich RW (1997) Allosteric gating of a large conductance Ca-activated K+ channel. *J Gen Physiol* **110**:257–281.

Danahay H, Fox R, Lilley S, Charlton H, Adley K, Christie L, Ansari E, Ehre C, Flen A, Tuvim MJ, et al. (2020) Potentiating TMEM16A does not stimulate airway mucus secretion or bronchial and pulmonary arterial smooth muscle contraction. *FASEB Bioadv* **2**:464–477.

Danielsson J, Perez-Zoghbi J, Bernstein K, Barajas MB, Zhang Y, Kumar S, Sharma PK, Gallos G, and Emala CW (2015) Antagonists of the TMEM16A calcium-activated chloride channel modulate airway smooth muscle tone and intracellular calcium. *Anesthesiology* **123**:569–581.

Du W, Bautista JF, Yang H, Diez-Sampedro A, You SA, Wang L, Kotagal P, Lüders HO, Shi J, Cui J, et al. (2005) Calcium-sensitive potassium channelopathy in human epilepsy and paroxysmal movement disorder. *Nat Genet* **37**:733–738.

Du X, Gao H, Jaffe D, Zhang H, and Gamper N (2018) M-type K^+ channels in peripheral nociceptive pathways. *Br J Pharmacol* **175**: 2158–2172.

Duncan RK (2005) Tamoxifen alters gating of the BK alpha subunit and mediates enhanced interactions with the avian beta subunit. *Biochem Pharmacol* **70**:47–58.

Enomoto A, Kimura H, Chairoungdua A, Shigeta Y, Jutabha P, Cha SH, Hosoyamada M, Takeda M, Sekine T, Igarashi T, et al. (2002) Molecular identification of a renal urate anion exchanger that regulates blood urate levels. *Nature* **417**:447–452.

Garcia-Calvo M, Knaus HG, McManus OB, Giangiacomo KM, Kaczorowski GJ, and Garcia ML (1994) Purification and reconstitution of the high-conductance, calcium-activated potassium channel from tracheal smooth muscle. *J Biol Chem* **269**:676–682.

Gessner G, Cui YM, Otani Y, Ohwada T, Soom M, Hoshi T, and Heinemann SH (2012) Molecular mechanism of pharmacological activation of BK channels. *Proc Natl Acad Sci USA* **109**:3552–3557.

Gessner G, Heller R, Hoshi T, and Heinemann SH (2007) The amiodarone derivative 2-methyl-3-(3,5-diiodo-4-carboxymethoxybenzyl)benzofuran (KB130015) opens large-conductance Ca2+-activated K+ channels and relaxes vascular smooth muscle. *Eur J Pharmacol* **555**:185–193.

González-Corrochano R, La Fuente J, Cuevas P, Fernández A, Chen M, Sáenz de Tejada I, and Angulo J (2013) Ca2+ -activated K+ channel (KCa) stimulation improves relaxant capacity of PDE5 inhibitors in human penile arteries and recovers the reduced efficacy of PDE5 inhibition in diabetic erectile dysfunction. *Br J Pharmacol* **169**:449–461.

Greenwood IA and Ohya S (2009) New tricks for old dogs: KCNQ expression and role in smooth muscle. *Br J Pharmacol* **156**:1196–1203.

Gribkoff VK, Lum-Ragan JT, Boissard CG, Post-Munson DJ, Meanwell NA, Starrett Jr JE, Kozlowski ES, Romine JL, Trojnacki JT, Mckay MC, et al. (1996) Effects of channel modulators on cloned large-conductance calcium-activated potassium channels. *Mol Pharmacol* **50**:206–217.

Gribkoff VK, Starrett Jr JE, Dworetzky SI, Hewawasam P, Boissard CG, Cook DA, Frantz SW, Heman K, Hibbard JR, Huston K, et al. (2001) Targeting acute ischemic stroke with a calcium-sensitive opener of maxi-K potassium channels. *Nat Med* **7**:471–477.

Haick JM and Byron KL (2016) Novel treatment strategies for smooth muscle disorders: targeting Kv7 potassium channels. *Pharmacol Ther* **165**:14–25.

Hashitani H and Brading AF (2003) Ionic basis for the regulation of spontaneous excitation in detrusor smooth muscle cells of the guinea-pig urinary bladder. *Br J Pharmacol* **140**:159–169.

Heinze C, Seniuk A, Sokolov MV, Huebner AK, Klementowicz AE, Szijártó IA, Schleifenbaum J, Vitzthum H, Gollasch M, Ehmke H, et al. (2014) Disruption of vascular Ca2+-activated chloride currents lowers blood pressure. *J Clin Invest* **124**:675–686.

Herrera GM, Heppner TJ, and Nelson MT (2000) Regulation of urinary bladder smooth muscle contractions by ryanodine receptors and BK and SK channels. *Am J Physiol Regul Integr Comp Physiol* **279**:R60–R68.

Hite RK, Tao X, and MacKinnon R (2017) Structural basis for gating the high-conductance Ca^{2+}-activated K^+ channel. *Nature* **541**:52–57.

Horrigan FT and Aldrich RW (2002) Coupling between voltage sensor activation, Ca2+ binding and channel opening in large conductance (BK) potassium channels. *J Gen Physiol* **120**:267–305.

Hoshi T, Tian Y, Xu R, Heinemann SH, and Hou S (2013a) Mechanism of the modulation of BK potassium channel complexes with different auxiliary subunit compositions by the omega-3 fatty acid DHA. *Proc Natl Acad Sci USA* **110**:4822–4827.

Hoshi T, Xu R, Hou S, Heinemann SH, and Tian Y (2013b) A point mutation in the human Slo1 channel that impairs its sensitivity to omega-3 docosahexaenoic acid. *J Gen Physiol* **142**:507–522.

Huang F, Zhang H, Wu M, Yang H, Kudo M, Peters CJ, Woodruff PG, Solberg OD, Donne ML, Huang X, et al. (2012) Calcium-activated chloride channel TMEM16A modulates mucin secretion and airway smooth muscle contraction. *Proc Natl Acad Sci USA* **109**:16354–16359.

Hull CA, Chu Y, Thanawala M, and Regehr WG (2013) Hyperpolarization induces a long-term increase in the spontaneous firing rate of cerebellar Golgi cells. *J Neurosci* **33**:5895–5902.

Kaczorowski GJ and Garcia ML (2016) Developing molecular pharmacology of BK channels for therapeutic benefit. *Int Rev Neurobiol* **128**:439–475.

Kilkenny C, Browne W, Cuthill IC, Emerson M, and Altman DG; NC3Rs Reporting Guidelines Working Group (2010) Animal research: reporting in vivo experiments: the ARRIVE guidelines. *Br J Pharmacol* **160**:1577–1579.

Kimm T, Khaliq ZM, and Bean BP (2015) Differential regulation of action potential shape and burst-frequency firing by BK and Kv2 channels in substantia nigra dopaminergic neurons. *J Neurosci* **35**:16404–16417.

Kshatri AS, Li Q, Yan J, Large RJ, Sergeant GP, McHale NG, Thornbury KD, and Hollywood MA (2017) Differential efficacy of GoSlo-SR compounds on BKα and BKα$\gamma_{1\text{-}4}$ channels. *Channels (Austin)* **11**:66–78.

Lai WS, Lin YY, Chu YH, Wang CH, and Wang HW (2013) Efficacy of fexofenadine in isolated rat tracheas. *Rhinology* **51**:376–380.

Latorre R, Castillo K, Carrasquel-Ursulaez W, Sepulveda RV, Gonzalez-Nilo F, Gonzalez C, and Alvarez O (2017) Molecular determinants of BK channel functional diversity and functioning. *Physiol Rev* **97**:39–87.

Lee US and Cui J (2009) Beta subunit-specific modulations of BK channel function by a mutation associated with epilepsy and dyskinesia. *J Physiol* **587**:1481–1498.

Liu Y, Zhang H, Huang D, Qi J, Xu J, Gao H, Du X, Gamper N, and Zhang H (2015) Characterization of the effects of Cl^- channel modulators on TMEM16A and bestrophin-1 Ca^{2+} activated Cl^- channels. *Pflugers Arch* **467**:1417–1430.

Lorca RA, Stamnes SJ, Pillai MK, Hsiao JJ, Wright ME, and England SK (2014) N-terminal isoforms of the large-conductance Ca^{2+}-activated K^+ channel are differentially modulated by the auxiliary β1-subunit. *J Biol Chem* **289**:10095–10103.

Ma Z, Lou XJ, and Horrigan FT (2006) Role of charged residues in the S1-S4 voltage sensor of BK channels. *J Gen Physiol* **127**:309–328.

Manville RW and Abbott GW (2018) Ancient and modern anticonvulsants act synergistically in a KCNQ potassium channel binding pocket. *Nat Commun* **9**:3845.

Martín P, Moncada M, Enrique N, Asuaje A, Valdez Capuccino JM, Gonzalez C, and Milesi V (2014) Arachidonic acid activation of BKCa (Slo1) channels associated to the β1-subunit in human vascular smooth muscle cells. *Pflugers Arch* **466**:1779–1792.

McCobb DP, Fowler NL, Featherstone T, Lingle CJ, Saito M, Krause JE, and Salkoff L (1995) A human calcium-activated potassium channel gene expressed in vascular smooth muscle. *Am J Physiol* **269**:H767–H777.

Meredith AL, Thorneloe KS, Werner ME, Nelson MT, and Aldrich RW (2004) Overactive bladder and incontinence in the absence of the BK large conductance Ca2+-activated K+ channel. *J Biol Chem* **279**:36746–36752.

Miner K, Labitzke K, Liu B, Wang P, Henckels K, Gaida K, Elliott R, Chen JJ, Liu L, Leith A, et al. (2019) Drug repurposing: the anthelmintics niclosamide and nitazoxanide are potent TMEM16A antagonists that fully bronchodilate airways. *Front Pharmacol* **10**:51.

Mushtaq Y (2014) The COPD pipeline. *Nat Rev Drug Discov* **13**:253.

Niu X, Qian X, and Magleby KL (2004) Linker-gating ring complex as passive spring and Ca(2+)-dependent machine for a voltage- and Ca(2+)-activated potassium channel. *Neuron* **42**:745–756.

Orio P, Rojas P, Ferreira G, and Latorre R (2002) New disguises for an old channel: MaxiK channel beta-subunits. *News Physiol Sci* **17**:156–161.

Passmore GM, Selyanko AA, Mistry M, Al-Qatari M, Marsh SJ, Matthews EA, Dickenson AH, Brown TA, Burbidge SA, Main M, et al. (2003) KCNQ/M currents in sensory neurons: significance for pain therapy. *J Neurosci* **23**:7227–7236.

Reinders MK, van Roon EN, Jansen TL, Delsing J, Griep EN, Hoekstra M, van de Laar MA, and Brouwers JR (2009) Efficacy and tolerability of urate-lowering drugs in gout: a randomised controlled trial of benzbromarone versus probenecid after failure of allopurinol. *Ann Rheum Dis* **68**:51–56.

Roddy E and Doherty M (2010) Epidemiology of gout. *Arthritis Res Ther* **12**:223.

Sanchez M and McManus OB (1996) Paxilline inhibition of the alpha-subunit of the high-conductance calcium-activated potassium channel. *Neuropharmacology* **35**: 963–968.

Schrøder RL, Strøbaek D, Olesen S-P, and Christophersen P (2003) Voltage-independent KCNQ4 currents induced by (+/-)BMS-204352. *Pflugers Arch* **446**:607–616.

Semenov I, Wang B, Herlihy JT, and Brenner R (2006) BK channel beta1-subunit regulation of calcium handling and constriction in tracheal smooth muscle. *Am J Physiol Lung Cell Mol Physiol* **291**:L802–L810.

Shao LR, Halvorsrud R, Borg-Graham L, and Storm JF (1999) The role of BK-type Ca2+-dependent K+ channels in spike broadening during repetitive firing in rat hippocampal pyramidal cells. *J Physiol* **521**:135–146.

Tao X, Hite RK, and MacKinnon R (2017) Cryo-EM structure of the open high-conductance Ca^{2+}-activated K^+ channel. *Nature* **541**:46–51.
Tao X and MacKinnon R (2019) Molecular structures of the human Slo1 K^+ channel in complex with β4. *eLife* **8**:e51409.
Tian Y, Heinemann SH, and Hoshi T (2019) Large-conductance Ca^{2+}- and voltage-gated K^+ channels form and break interactions with membrane lipids during each gating cycle. *Proc Natl Acad Sci USA* **116**:8591–8596.
Tian Y, Ullrich F, Xu R, Heinemann SH, Hou S, and Hoshi T (2015) Two distinct effects of PIP2 underlie auxiliary subunit-dependent modulation of Slo1 BK channels. *J Gen Physiol* **145**:331–343.
Vaithianathan T, Bukiya A, Liu J, Liu P, Asuncion-Chin M, Fan Z, and Dopico A (2008) Direct regulation of BK channels by phosphatidylinositol 4,5-bisphosphate as a novel signaling pathway. *J Gen Physiol* **132**:13–28.
Valverde MA, Rojas P, Amigo J, Cosmelli D, Orio P, Bahamonde MI, Mann GE, Vergara C, and Latorre R (1999) Acute activation of Maxi-K channels (hSlo) by estradiol binding to the beta subunit. *Science* **285**:1929–1931.
Vang A, Mazer J, Casserly B, and Choudhary G (2010) Activation of endothelial BKCa channels causes pulmonary vasodilation. *Vascul Pharmacol* **53**:122–129.
Walter-Sack I, de Vries JX, Ittensohn A, Kohlmeier M, and Weber E (1988) Benzbromarone disposition and uricosuric action; evidence for hydroxilation instead of debromination to benzarone. *Klin Wochenschr* **66**:160–166.
Webb TI, Kshatri AS, Large RJ, Akande AM, Roy S, Sergeant GP, McHale NG, Thornbury KD, and Hollywood MA (2015) Molecular mechanisms underlying the effect of the novel BK channel opener GoSlo: involvement of the S4/S5 linker and the S6 segment. *Proc Natl Acad Sci USA* **112**:2064–2069.
Womack MD, Hoang C, and Khodakhah K (2009) Large conductance calcium-activated potassium channels affect both spontaneous firing and intracellular calcium concentration in cerebellar Purkinje neurons. *Neuroscience* **162**:989–1000.
Yan J and Aldrich RW (2010) LRRC26 auxiliary protein allows BK channel activation at resting voltage without calcium. *Nature* **466**:513–516.
Yang Y, Li PY, Cheng J, Mao L, Wen J, Tan XQ, Liu ZF, and Zeng XR (2013) Function of BKCa channels is reduced in human vascular smooth muscle cells from Han Chinese patients with hypertension. *Hypertension* **61**:519–525.
Yellen G (2002) The voltage-gated potassium channels and their relatives. *Nature* **419**:35–42.
Yusifov T, Savalli N, Gandhi CS, Ottolia M, and Olcese R (2008) The RCK2 domain of the human BKCa channel is a calcium sensor. *Proc Natl Acad Sci USA* **105**:376–381.
Zavaritskaya O, Dudem S, Ma D, Rabab KE, Albrecht S, Tsvetkov D, Kassmann M, Thornbury K, Mladenov M, Kammermeier C, et al. (2020) Vasodilation of rat skeletal muscle arteries by the novel BK channel opener GoSlo is mediated by the simultaneous activation of BK and K_v 7 channels. *Br J Pharmacol* **177**:1164–1186.
Zhang C-H, Li Y, Zhao W, Lifshitz LM, Li H, Harfe BD, Zhu M-S, and ZhuGe R (2013) The transmembrane protein 16A Ca(2+)-activated Cl- channel in airway smooth muscle contributes to airway hyperresponsiveness. *Am J Respir Crit Care Med* **187**:374–381.
Zhang G, Geng Y, Jin Y, Shi J, McFarland K, Magleby KL, Salkoff L, and Cui J (2017) Deletion of cytosolic gating ring decreases gate and voltage sensor coupling in BK channels. *J Gen Physiol* **149**:373–387.
Zhang G, Huang SY, Yang J, Shi J, Yang X, Moller A, Zou X, and Cui J (2010) Ion sensing in the RCK1 domain of BK channels. *Proc Natl Acad Sci USA* **107**:18700–18705.
Zhang J and Yan J (2014) Regulation of BK channels by auxiliary gamma subunits. *Front Physiol* **5**:401.
Zheng Y, Xu H, Zhan L, Zhou X, Chen X, and Gao Z (2015) Activation of peripheral KCNQ channels relieves gout pain. *Pain* **156**:1025–1035.

Address correspondence to: Dr. Yani Liu, Department of Pharmacology, School of Pharmacy, Qingdao University Medical College, #1 Ningde Road, Qingdao 266073, China. E-mail: liuyani@qdu.edu.cn; or Prof. KeWei Wang, Department of Pharmacology, School of Pharmacy, Qingdao University Medical College, #1 Ningde Road, Qingdao 266073, China. E-mail: wangkw@qdu.edu.cn